ELSEVIER

Atmospheric Environment 38 (2004) 6855–6866

ATMOSPHERIC ENVIRONMENT

www.elsevier.com/locate/atmosenv

Evaluation of a micrometeorological mass balance method employing an open-path laser for measuring methane emissions

R.L. Desjardins[a,*], O.T. Denmead[b], L. Harper[c], M. McBain[a], D. Massé[d], S. Kaharabata[a]

[a]*Agriculture and Agri-Food Canada, Research Branch, K.W. Neatby Building, 960 Carling Avenue, Ottawa, ON, Canada K1A 0C6*
[b]*CSIRO Land and Water, GPO Box 1666, Canberra ACT 2601, Australia*
[c]*Agriculture Research Service, United States Department of Agriculture, 1420 Experiment Station Road, Watkinsville, GA 30677, USA*
[d]*Agriculture and Agri-Food Canada, Research Branch, 2000 Route 108 East, P.O. Box 90, Lennoxville, QC, Canada J1M 1Z3*

Received 29 March 2004; accepted 23 August 2004

Abstract

In trials of a mass balance method for measuring methane (CH_4) emissions, sonic anemometers and an open-path laser were used to measure the transport of CH_4 released from a ground-level source across a downwind face 50 m long and 6 m high. Release rates matched emissions expected from dairy herds of 2 to 40 cows. The long laser path permitted inferences from measurements in only two planes, one upwind and one downwind, while the fast-response instruments allowed calculation of instantaneous horizontal fluxes rather than fluxes calculated from mean wind speeds and mean concentrations. The detection limit of the lasers was 0.02 ppmv, with the separation between the transmitters and reflectors being about 50 m. The main conclusions from the 23 trials were: (1) Emissions calculated from mean wind speeds and concentrations overestimated the true emissions calculated from instantaneous measurements by 5%. (2) Because of small changes in methane concentration, the minimum sample size in animal trials would be 10 dairy cows, producing about 40 mg $CH_4\,s^{-1}$. (3) For release rates greater than 40 mg $CH_4\,s^{-1}$ and with sufficient replication, the technique could detect a change in production rate of 9% ($P <= 0.05$). (4) Attention to perceived weaknesses in the present technique should help towards detecting changes of 5%.
Published by Elsevier Ltd.

Keywords: Anthropogenic methane emissions; Mean horizontal flux; Recovery rates; Open-path laser-based gas analyzers; Mass balance method

1. Introduction

Anthropogenic emissions of methane (CH_4) are estimated to contribute 20% of the world's greenhouse gas emissions (IPCC, 2001). About 29% of the anthropogenic CH_4 emissions come from enteric fermentation in ruminant animals (notably cattle and sheep). Reducing these emissions is obviously important if countries hope to meet their obligations as a signatory to Kyoto. Various reduction measures have been proposed, but our ability to detect relatively small reductions of, say, 10–20% remains a challenge. Such differences are very

*Corresponding author. Tel.: +1 613 759 1522; fax: +1 613 759 1432.
E-mail address: desjardins@agr.gc.ca (R.L. Desjardins).

1352-2310/$ - see front matter Published by Elsevier Ltd.
doi:10.1016/j.atmosenv.2004.09.008

significant for either inventory, regulatory or mitigation purposes.

Inventories of CH_4 production by ruminants, such as those proposed by the IPCC (1996) (Tier 1), are based largely on measurements with confined animals in chambers (e.g., Blaxter and Clapperton, 1965; Miller and Koes, 1988). Tier 2 proposes to estimate CH_4 production from knowledge of animal type, feed intake and feed quality. Given the wide variations that exist in animal types and feedstuffs, there is a need to assess the applicability of such relationships at local scales.

Johnson et al. (1994) suggest that because a chamber is an artificial, constrained environment, the extent to which chamber results can be extrapolated to animals in production environments (range, pasture, feedlots, etc.) with a full range of normal animal activities is open to question. Further, it will not always be possible to test mitigation techniques that involve animal management practices in chambers. Johnson et al. (1994) developed an alternate method for measuring CH_4 emissions, in which a capsule containing sulphur hexafluoride (SF_6) is placed in the rumen. The ratio of CH_4 to SF_6 in the animal's breath is then used in conjunction with the known rate of SF_6 diffusion from the capsule to calculate CH_4 production rates. The animals are able to perform most of their normal activities but they must be brought in from the pasture several times daily. This means that the sensor equipment must be removed and replaced, causing alterations in their usual activity. Another approach has been to graze animals in a portable wind-tunnel. Methane production is calculated from changes in the CH_4 concentration of air entering and leaving the chamber (Lockyer and Jarvis, 1995). Both of these latter techniques, however, add some measure of animal stress above normal field grazing and the sample sizes are small.

Micrometeorological techniques appropriate for measuring gas emissions from large grazed areas have also been employed. Judd et al. (1999) used a flux-gradient technique to measure CH_4 emissions from grazing sheep which populated the entire upwind fetch. Fencing was arranged so as to have a uniform stocking rate of 20 sheep ha^{-1}, extending hundreds of metres upwind and laterally. A similar flux-gradient approach as well as convective boundary layer analysis has been used by Denmead et al. (2000) to measure emissions from grazed areas several km^2 in extent. These micrometeorological methods, however, are on too large a scale to be employed for measuring CH_4 emissions from animals in many on-farm situations.

Recently, Venkatram (2004) discussed a method of estimating emissions through horizontal fluxes that would be suitable for smaller-scale measurements. Denmead et al. (1998), Harper et al. (1999) and Leuning et al. (1999) also describe mass balance methods developed for this purpose. With this technique, known as a micrometeorological mass difference (MMD) method, they could calculate net emissions from animals in small, bounded areas from the difference in the amounts of CH_4 carried across the upwind and downwind planes of the test area. Measurements of the horizontal flux of CH_4, the product of wind speed u and concentration ρ were made on all four boundaries of the rectilinear test area. These measurements were integrated over the length and height of the gas sampling lines to give the net fluxes into and out of the test space. In those applications, sampling lines at four heights extended for the entire length of each boundary.

The mean horizontal flux is given by the mean of the instantaneous fluxes, i.e. by $\overline{u\rho}$. However, in most experiments in which the MMD method has been applied, fluxes have been determined as the product of mean wind speed and mean concentration, i.e. as $\bar{u}\bar{\rho}$. This treatment, however, ignores terms in the turbulent transport equation since the instantaneous wind speeds and concentrations represent the sums of time means and deviations from those means: $u = \bar{u} + u'$ and $\rho = \bar{\rho} + \rho'$, the primes denoting the deviations from the means. Thus $\overline{u\rho} = \bar{u}\bar{\rho} + \overline{u'\rho'}$. The last term represents turbulent diffusion in the upwind direction, along the concentration gradient. In previous applications employing $\bar{u}$ and $\bar{\rho}$, the practice has been to approximate the diffusive term by an empirical amount based on theory and experiment, which suggest amounts of 5–15% of the horizontal flux (Leuning et al., 1985; Denmead et al., 1998). In the present study, part of the uncertainty in the instantaneous wind speed measurements has been removed by the use of sonic anemometers, and uncertainties in concentration measurements have been overcome through the application of open-path laser-based gas analyzers. Because of the long measuring path possible with the open-path laser, only one upwind and one parallel downwind boundary need be considered, which makes it possible to simplify the MMD method.

This paper provides the results of a study that was designed to evaluate the accuracy of the simplified MMD technique with the open-path laser technology. The technique is applicable to a large number of on-farm scenarios including emissions from animals, manure piles and lagoons.

2. Materials and methods

2.1. Site and environmental conditions

Trials of the method were conducted in a field within the Central Experimental Farm of Agriculture and Agri-Food Canada (AAFC) in Ottawa, Canada in September 2002. The field was essentially flat with no

significant obstructions to wind flow for hundreds of metres round about. The vegetation was short grass, about 0.2 m high. The soil was mostly dry and no significant rainfalls occurred over the experimental period. Thus most of the heat transfer at the surface was as sensible heat. Coupled with light to moderate wind speeds, this often led to highly unstable conditions with the Monin–Obukhov length between −1 and −10 m. Only a few trials were conducted in stable conditions at night.

2.2. Experimental set-up

Because of the long measuring distance possible with the open-path laser, only one upwind and one parallel downwind boundary need be considered. Note that in order to avoid the need for another instrument array upwind, which would have been prohibitively expensive and would have entailed a lot more data analysis, the background CH_4 concentrations were measured 15 min before and after releasing known concentrations of CH_4. Provided the downwind measuring path is long enough to traverse the entire width of the emitted gas cloud and the horizontal wind speed for a given height $u(z)$ is uniform across the path, it follows that the MMD method can be modified to be

$$F = X \int_0^Z \overline{U_n(\rho_{CH_4,z,d} - \rho_{CH_4,z,b})}\,dz, \quad (1)$$

where X is the length of the laser path (separation (m) between transmitter head and reflector array), U_n is the wind speed normal to the boundaries, ρ is the scalar concentration and the subscripts d and b denote downwind and background, respectively.

The modified (simplified) MMD method was tested by using it to determine the recovery of CH_4 released at various known rates upwind (Fig. 1). The laser path length X was set at 50.5 m. Wind speeds, wind directions and CH_4 concentrations were measured at six heights with the top one at 6 m. Instrumentation and sampling procedures are detailed in subsequent paragraphs. Releases of CH_4 were made from a grid (3×3 m) constructed from 17.5 mm (inner diameter (ID)) PVC tubing with 16 (0.8 mm ID) holes drilled at approximately 1 m intervals. Methane of 99% purity was fed to the grid from a cylinder through a Thermo Systems Inc. (TSI) mass flow meter. In most of the releases, the TSI mass flow meter was placed in line with an MKS Instruments Inc. (MKS) mass flow controller (Fig. 1). Usually the grid was positioned near the mid-point of the laser path, with its centre at 10–12 m upwind of the line (Fig. 1). Release rates were varied to cover a range in the number of animals of dairy farm operations. Releases were usually about 30 min in duration.

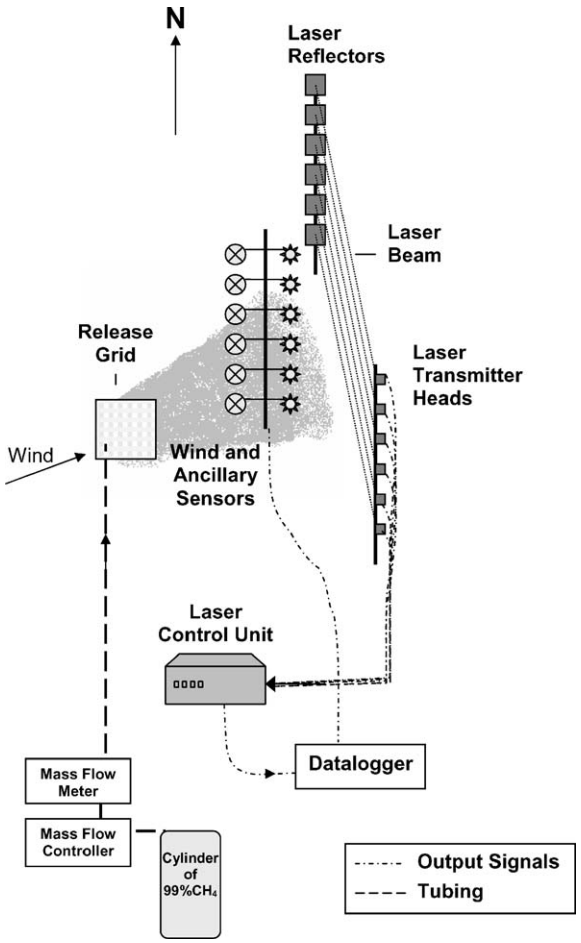

Fig. 1. Schematic representation of the modified MMD method set-up.

2.3. Open-path laser

A Boreal Laser Inc. GasFinder MC system was used. It comprises a central control unit housing the laser diode source, detector signal processing and microcomputer subsystems. With this system, a tuneable infrared laser diode is used to produce a collimated beam of light that is transferred to a transmitter head via fibre-optic cable. The laser light emitted from the transmitter head propagates through the atmosphere to a compound mirror (retroreflector) and returns to the transmitter head where it is focused onto a photodiode source. The return signal is then transmitted back to the main control unit via coaxial cable and is processed to determine the CH_4 concentration. The measurement wavelength for the CH_4 GasFinder MC unit is 1653 nm and because the unit is designed to scan over a small spectral range (typically less than a few Angstroms), cross interference with other gas species is not a problem (Bauer, 2004, personal communication).

The system can support eight laser transmitter heads with a path length (separation (m) between transmitter heads and reflector array) of several hundred metres. In our application, six laser transmitter heads were used with a path length of 50.5 m. The resolution of the system is given by the manufacturers as 1 ppmm, which for our system corresponds to a detection limit of 0.02 ppmv. The transmitters and reflectors were tower-mounted at the same heights as the sonic anemometers (Fig. 1).

2.4. Sonic anemometers

Six two-dimensional Vaisala WAS425 ultrasonic wind sensors were used to measure horizontal wind speed and direction. They were mounted on a tower about 3 m West (W) of the mid-point of the laser line, as shown in Fig. 1, directly in front of the release grid. In early releases (1–9), the sensors were mounted at 0.9, 2, 3, 4, 5 and 6 m above the ground and in later releases (10–23) at 0.4, 0.9, 2, 3, 4 and 6 m above the ground.

Wind directions relative to magnetic North (N) α (degrees) were measured by the sonic anemometers. The laser path was oriented 20°W of N. The algorithm for computing wind speeds normal (U_n) to the laser path is then

$$U_n = u \sin(\alpha - 160). \quad (2)$$

Subsequent data analysis involved an examination of the effects of wind direction on recovery. Data were discarded whenever the wind direction was such that the released CH_4 would be carried outside particular segments of the laser path, as illustrated in Fig. 2. The algorithm employed included data if

$$\left\{270 + \beta - \tan^{-1}\left[\frac{(X/2 - X_c)}{X_u}\right]\right\} < (\alpha + 20)$$
$$< \left\{270 - \beta + \tan^{-1}\left[\frac{(X/2 + X_c)}{X_u}\right]\right\}, \quad (3)$$

where X_c and X_u are the crosswind and upwind distances from the centre of the laser path to the centre of the source grid.

2.5. Data collection procedure

In order to apply Eq. (1), corresponding wind speeds and concentrations must be measured simultaneously. In our application, wind speed could be logged at 10 Hz, but the central control unit on the laser cycled around the individual transmitters at a frequency of 0.3 Hz. Hence, a logging programme was devised to synchronize the collection of the two signals. The trigger for data collection was the switch from one transmitter to the next. In a 30 min release, some 80 complete profile scans with matching wind speed and concentration measurements at each height were recorded.

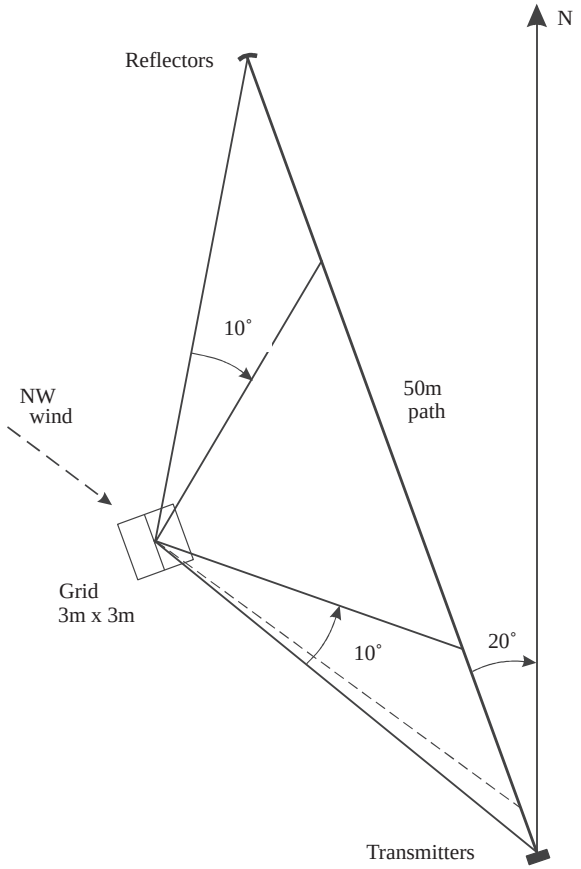

Fig. 2. Simplified schematic representation of the modified MMD set-up showing the laser line with exclusion angles of 10° drawn in. The trajectory of a NW wind (dashed line) could carry the methane outside the segment defined by the exclusion angles and the corresponding wind speeds and concentrations would be excluded from the data set for that release.

2.6. Ancillary measurements

Additional measurements were made of profiles of wind speed and temperature close to the ground using sensitive cup anemometers and aspirated thermocouples. The instruments were mounted at heights of 0.2, 0.4, 0.6, 0.8, 1.6 and 2.7 m above the ground (Fig. 1). These enabled calculation of the Monin–Obukhov length L, the friction velocity u_* and the sensible heat flux H, using the integrated forms of the stability functions developed by Paulson (1970) for unstable conditions and Thom (1975) for stable conditions.

2.7. Comparison of mass flow meter and mass flow controller

The TSI mass flow meter provides the apparent volume flow rate ($L\,min^{-1}$) for air corrected to a

temperature of 21 °C. That flow must be multiplied by a gas correction factor of 0.71 to obtain the flow rate for CH_4, also correct at a temperature of 21 °C. The MKS mass flow controller has a gas correction adjustment control to allow the instrument to read correctly for any particular gas. Also, the controller provides the volume flow rate corrected to a temperature of 0 °C and an atmospheric pressure of 760 mm Hg. This allows the mass flow to be calculated simply through the gas constant.

The algorithm used to convert the MKS indicated volumetric flow rate V ($L\,min^{-1}$) to mass flow rate M ($mg\,s^{-1}$), which also allows for the fact that the gas released from the cylinder was 99% CH_4 in air, was

$$M = 1000\,V\left(\frac{16}{22.4}\right)\left(\frac{0.99}{60}\right). \quad (4)$$

The MKS unit was calibrated in the laboratory, but the temperature conditions were indeterminate and the factory calibration was employed throughout. An empirical field calibration of the TSI instrument was made by regressing its indicated flow rate on that of the MKS flow controller during 21 releases. The regression equation gave

$$V_{MKS} = 0.4808\,V_{TSI};\ r^2 = 0.98. \quad (5)$$

For most releases, MKS flow rate data were used; however, in seven early releases when only TSI data were available, Eq. (5) was used to estimate the MKS flow rate.

2.8. Calculating recovery rates

This proceeded in two stages. The volumetric CH_4 concentrations c (ppmv) indicated by the laser system were converted to CH_4 densities, ρ_{CH_4} ($mg\,m^{-3}$), through the algorithm

$$\rho_{CH_4} = c\rho_a\left(\frac{16}{28.97}\right) \quad (6)$$

with 16 and 28.97 being the molecular weights of CH_4 and air, and ρ_a the density of air at field temperature ($kg\,m^{-3}$). Following List (1951), ρ_a is given by

$$\rho_a = \frac{0.34838p}{T_v}, \quad (7)$$

where p denotes atmospheric pressure (hPa) and T_v the adjusted virtual temperature (K). In the absence of on-site measurements of pressure and humidity, p was assumed to be 1013.2 hPa and T_v equal to the temperature measured at 2.7 m.

The second stage in the calculation was to evaluate the integral in Eq. (1). This was done using the trapezoidal rule, viz.,

$$\int_{z_0}^{z_n} y\,dz = \int_{z_0}^{z_1} y\,dz + \int_{z_1}^{z_2} y\,dz + \cdots + \int_{z_{n-1}}^{z_n} y\,dz$$
$$= \frac{z_1}{2}(y_0 + y_1) + \frac{(z_2 - z_1)}{2}(y_1 + y_2) + \cdots + \frac{(z_n - z_{n-1})}{2}(y_{n-1} + y_n) \quad (8)$$

and was initially completed using $z = 0.9, 2, 3, 4, 5, 6$ m for releases 1–9, $z = 0.4, 0.9, 2, 3, 4, 6$ m for releases 10–23.

Two additional techniques were also used to evaluate Eq. (1): an interpolation and a regression method. Following a similar method as that of Wagner-Riddle et al. (2004), the "interp1" and "linear-in-the-parameters" functions in MATLAB software were used to generate interpolated and regressed profiles based on real measurement values (from heights 0.9, 2, 3, 4, 5, 6 m for releases 1–9, and heights 0.4, 0.9, 2, 3, 4, 6 m for releases 10–23). The mean product of wind speed multiplied by the change in gas concentration ($\overline{U_n(\rho_d - \rho_b)}$) was evaluated at each sampling height prior to being used in both the interpolation and regression models. Therefore the output from each model was a series of data points ($\overline{U_n(\rho_d - \rho_b)}$), generated for heights corresponding to 0–6 m at 0.01 m intervals. These data points were then used to calculate the integral in Eq. (1). The three integration techniques are compared in Section 3.4.

3. Results and discussion

3.1. Comparison of anemometers

Fig. 3a shows ensemble-averaged wind profiles for the sonic anemometers and includes the corresponding low-level profiles measured by the cup anemometers. The profiles indicated by the sonic anemometers are slightly irregular in shape, whereas those indicated by the cups have the expected smooth log shape. This may be simply because the sonic profiles extend to greater heights where they are influenced by distant upwind obstructions. The sonic and cup anemometer profiles appear to be in fair agreement in releases 1–9, but do diverge slightly between 1 and 3 m height in releases 10–23 (Fig. 3a). This could be due to errors in the readings of the cup anemometers in the light wind that prevailed during the latter releases.

3.2. Background concentrations

In Eq. (1), the differential CH_4 density is the increase above background. The background concentrations for each release were taken to be the means of those recorded for 15 min just before and 15 min just after the

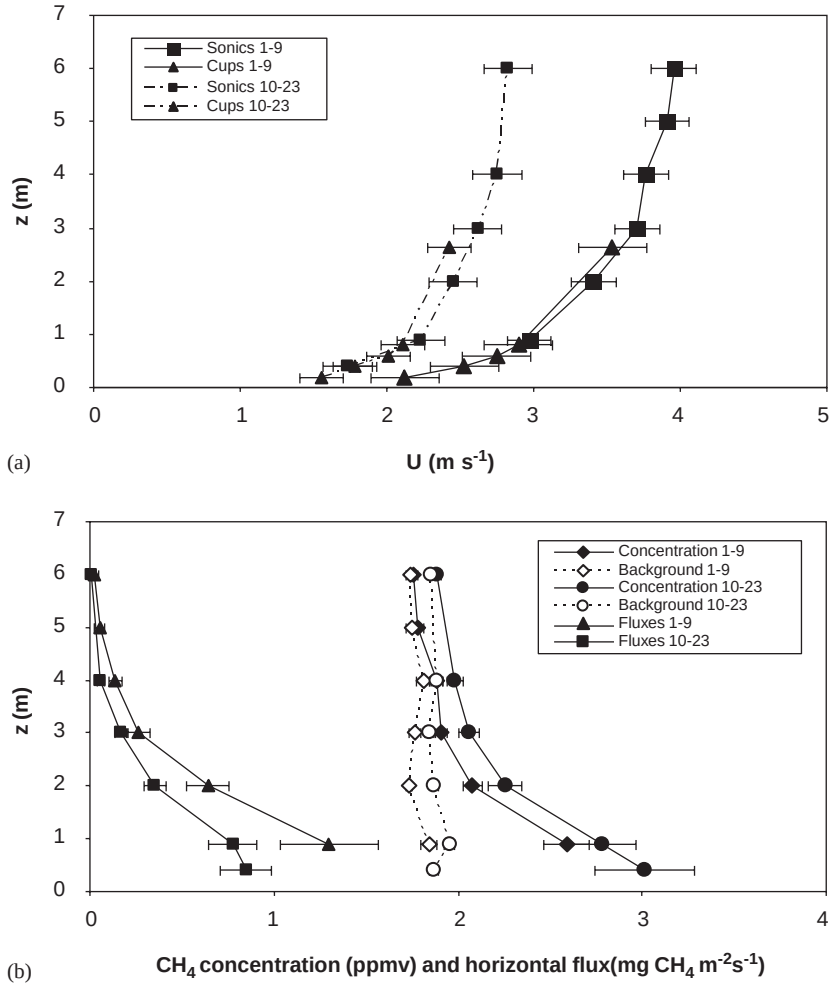

Fig. 3. (a) Ensemble-averaged wind speeds measured by cup and sonic anemometers during releases 1–9 and 10–23, and the corresponding standard errors. (b) Ensemble-averaged backgrounds, concentrations and horizontal fluxes for releases 1–9 and 10–23 and the corresponding standard errors.

release. Averaging the "before" and "after" background concentrations removed the slow environmental drift that we observed in the background concentrations. Fig. 3b shows the ensemble-averaged background concentrations, the concentrations at the laser path during release, and the horizontal fluxes calculated by Eq. (1) for releases 1–9 and 10–23. The overall mean background is 1.84 ppmv, which is consistent with the global value for 1998 of 1.75 ppmv (IPCC, 2001) allowing for a slightly higher concentration in the northern hemisphere and an annual increase of about 0.01 ppmv. The overall mean concentration along the laser path for all releases was only 2.21 ppmv, just 0.37 ppmv above background. In one release, the mean difference in concentration was only 0.04 ppmv. While detection of such small differences is within the nominal sensitivity of the laser system (0.02 ppmv), these figures indicate the precision required in the technique. It requires accurate determination of small differences between relatively large numbers.

Table 1 shows 15-min average background CH_4 concentrations measured by six of the laser transmitter heads before and after four successive releases along with the corresponding differences in CH_4 concentrations. It is evident that many of the concentration differences are often close to, or more than the nominal sensitivity of the laser system. Some of the larger differences demonstrate that periodically some unexplained variances in the background CH_4 concentration were observed with the laser system. These differences tended to affect one head at a time and had a relatively minor impact on the CH_4 flux estimates. Even though each transmitter head is connected to the same laser diode source, mean background concentrations amongst

Table 1
An example of 15-min average before and after (release) background CH_4 concentrations (ppmv) for laser transmitter heads 1–6

	Mean CH_4 conc. (ppmv) (head 1)	Mean CH_4 conc. (ppmv) (head 2)	Mean CH_4 conc. (ppmv) (head 3)	Mean CH_4 conc. (ppmv) (head 4)	Mean CH_4 conc. (ppmv) (head 5)	Mean CH_4 conc. (ppmv) (head 6)
Before	1.889	1.97	1.913	1.923	1.995	1.919
After	1.853	1.94	1.892	1.826	1.932	1.917
Difference ± s.d.	0.036 ± 0.037	0.030 ± 0.106	0.021 ± 0.068	0.097 ± 0.044	0.063 ± 0.034	0.002 ± 0.042
Before	1.853	1.94	1.892	1.826	1.932	1.917
After	1.833	1.894	1.841	1.863	1.865	1.794
Difference ± s.d.	0.020 ± 0.027	0.046 ± 0.034	0.051 ± 0.028	−0.037 ± 0.031	0.067 ± 0.040	0.123 ± 0.035
Before	1.833	1.894	1.841	1.863	1.865	1.794
After	1.773	1.843	1.796	1.737	1.836	1.809
Difference ± s.d.	0.020 ± 0.027	0.051 ± 0.021	0.045 ± 0.030	0.126 ± 0.024	0.029 ± 0.039	−0.015 ± 0.036
Before	1.801	1.872	1.787	1.792	1.841	1.876
After	1.848	1.894	1.847	1.846	1.836	1.854
Difference ± s.d.	−0.047 ± 0.021	−0.022 ± 0.023	−0.060 ± 0.024	−0.054 ± 0.026	0.005 ± 0.050	0.022 ± 0.032
Overall average difference ± s.d. (R1–R23)	0.022 ± 0.033	0.015 ± 0.036	0.012 ± 0.026	0.023 ± 0.030	0.014 ± 0.034	0.006 ± 0.030

For each release, the differences before and after concentrations (ppmv) and standard deviations are given. Data are selected from releases 13–16, respectively, and are fairly representative of all releases. The average difference and standard deviation between before and after concentrations for all releases (R1–R23) are also given.

the six laser transmitter heads were not expected to be the same as they use different optical cables and they were not adjusted to read the same. The positive overall average differences between before and after background concentrations (R1–R23) are likely because of the fact that the surrounding city is a source area of CH_4 (Table 1). Concentrations near the ground increased in the stable conditions overnight and decreased in the unstable conditions by day as the mixed layer grew. Most of our measurements were made during daylight hours when background concentrations were decreasing.

3.3. Mean uρ vs. the product of the means of u and ρ

Fig. 4 compares integrated horizontal fluxes calculated by substituting $\overline{U_n(\rho_{CH_4,z,d} - \rho_{CH_4,z,b})}$ for $\overline{U_n}(\overline{\rho_{CH_4,z,d}} - \overline{\rho_{CH_4,z,b}})$ in evaluating Eq. (1) in all the acceptable releases (trapezoidal rule). As indicated, $(\bar{u}\bar{\rho})$ overestimates the true flux given by $\overline{u\rho}$. In our application, the overestimation is very close to 5%. The tightness of the correlation between the fluxes computed by both methods ($r^2 = 0.996$) indicates that cup anemometers could have been used quite successfully in place of sonic anemometers without any significant loss in precision, provided that the 5% correction was applied.

During the releases there were no obstructions to wind flow and the tracer gas source was close to the laser path. Given the homogeneous site, it was safe to assume horizontally homogeneous turbulence and as a result the differences between u at a point and u averaged along the laser path were most likely random. Since the errors associated with u were not correlated with time variations in ρ_{CH_4}, one can assume the error introduced by using a point value of horizontal wind speed (u_p) multiplied by a line averaged gas concentration (ρ_a) would be negligible over sufficient time averaging (e.g. 30 min). Also, in our application the average plume width at the laser path was estimated to be about 13 m. Based on the spectral characteristics of surface layer turbulence obtained by Kaimal et al. (1972) and Desjardins et al. (1978), it was estimated that 80–90% of the horizontal velocity variance corresponded to a length scale greater than 6.5 m (given the anemometer tower was positioned in the middle of the emitting gas cloud). These two points confirm that we could measure $\overline{u\rho}$ with this technique with a reasonable degree of confidence. In the absence of surface homogeneity, these assumptions may not be applicable and in this case it would be necessary to obtain an average of the instantaneous horizontal wind speed along each laser path.

3.4. Recoveries

A comparison of the recovery rates calculated using the trapezoidal, interpolation and regression method showed that overall (average of 23 releases)

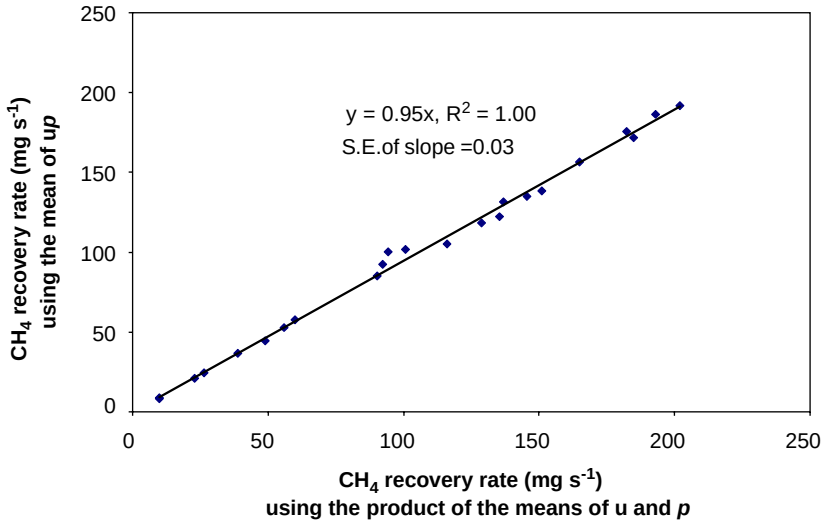

Fig. 4. Comparison of integrated horizontal fluxes calculated by substituting mean horizontal fluxes $\overline{U_n(\rho_{CH_4,z,d} - \rho_{CH_4,z,b})}$, for instantaneous horizontal fluxes, $\overline{U_n(\rho_{CH_4,z,d} - \rho_{CH_4,z,b})}$, in evaluating Eq. (3) for all the acceptable releases and an exclusion angle of 10°.

each method produced relatively similar results. The trapezoidal, interpolation and regression methods overestimated the release rates by an average of ~4%, ~5% and ~6%, respectively (based on a 10° exclusion angle). It is believed that the overestimation of the release rates from each of these methods was directly related to inadequate sampling of the high flux region below 0.9 m during releases 1–9. In particular, the lack of data in the high flux region would have increased the probability that the profiles generated by the interpolation and regression models were unrepresentative of the true in-situ profiles. This in turn would have increased the error in the CH_4 flux estimation.

Recovery rates for releases 1–9, calculated using the interpolation and regression methods, exceeded the release rates by an average of 14% and 16%, respectively. Recovery rates calculated using the trapezoidal method, however, only exceeded release rates by less than 5%. For releases 10–23, the recovery rates calculated using the trapezoidal, interpolated and regression methods showed much better agreement and were on average 105%, 98% and 102%, respectively, of the actual release rates. It is important to note that these results suggest that future testing of the interpolation and regression methods is warranted. Overall, it was decided that because of the variation in the interpolation and regression results, as well as the increased complexity involved in the data processing, subsequent data analysis would include only the recovery rates that were calculated using the trapezoidal method. The following paragraphs examine the effects of various factors on these recovery rates.

Fig. 5 shows the comparisons of recovery (trapezoidal method) and release rates in all acceptable releases. Overall, the agreement is good. Regression analysis of the 23 acceptable releases in the trial gave the following result: recovery rate = 1.05 × release rate; $r^2 = 0.91$. The fact that, on average, recovery slightly exceeded release could indicate an error in the purity of CH_4 in the release cylinder, an error in the calibration of the mass flow controller, errors in the calibrations of the laser/anemometers, or insufficient detail in the concentration and wind speed profiles. With regard to this last point, it can be seen in the ensemble profiles in Fig. 3b that there was inadequate sampling of the high flux region below 0.9 m in the early releases. Other possible causes for disagreement include wind direction, the effect of atmospheric stability on the height of the gas cloud and the buoyancy of CH_4.

3.5. Exclusion angle

The sonic anemometers were located 3 m upwind of the laser path. Although the anemometer at any particular height and the corresponding concentration were measured simultaneously, there was a time lag, typically of 1–2 s, between a parcel of air passing the anemometer and passing the laser line. Hence, it was possible for the trajectory of the parcel to change direction in that time. Also, we expect some lateral dispersion of the cloud generated by the release. Both these considerations and shifts in the mean wind direction during the release necessitated a procedure to eliminate data when wind directions were outside certain preset limits. The effects of changing the limits on

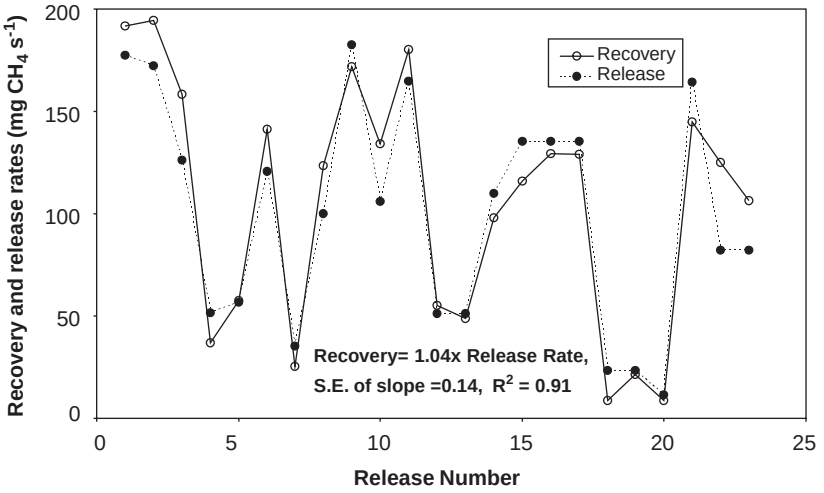

Fig. 5. Recovery and release rates in all acceptable releases. Recoveries are for the integrated instantaneous horizontal fluxes and an exclusion angle of 10°.

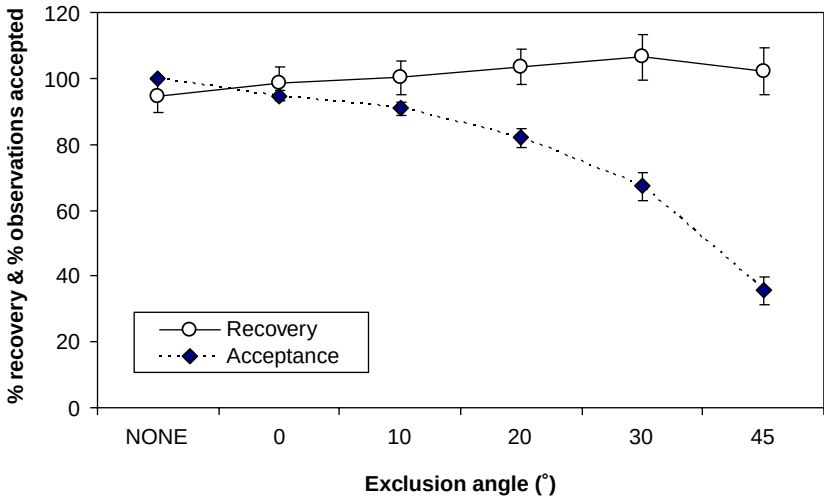

Fig. 6. Recoveries and their standard errors (expressed as percentages of release rate), and observations accepted with standard errors (expressed as a percentage of available observations) for various exclusion angles.

recovery of the released CH_4 were examined by applying condition (3). Recoveries were calculated for β values of 0° (exclude all trajectories carrying gas outside the laser line), 10°, 20°, 30° and 45°. We can note that for a typical placement of the grid with its centre 12 m upwind and 5 m crosswind from the centre of the laser line, these limits would restrict the acceptable laser path length to 50, 33, 23, 16 and 8 m, respectively.

The effects of exclusion angle on the recovery rate and the numbers of runs accepted as it was varied from none (no data excluded) to 0° and 10° are shown in Fig. 6. As expected, recoveries increased as the exclusion angle increased, while the proportion of acceptable observations decreased. An exclusion angle of 10° would seem to be a reasonable criterion at least in these trials. It gave a mean recovery of 100% with a 5% confidence interval of $\pm 10\%$ and excluded only 9% of the data. The recoveries reported above and in subsequent paragraphs are for this β. We note that if a longer path (e.g. 100 m) was used in release trials like these, it would not be as necessary to invoke an exclusion angle.

3.6. Effects of atmospheric stability

The height of the gas cloud depends on atmospheric stability. Fig. 7 illustrates this with two examples from the present study. Release rates were similar in both examples, 183 mg $CH_4\,s^{-1}$ in release 9 and 165 mg

$CH_4\,s^{-1}$ in release 11. The centre of the release grid was 12 m upwind in both cases, but release 9 was made near dusk in near neutral conditions ($L = -430$ m) while release 11 was made the next day in highly unstable conditions ($L = -3.5$ m). In release 9, there was some CH_4 enrichment up to a height of 3 m and all the horizontal transport of CH_4 occurred below that height, but in release 11 enrichment and horizontal transport occurred up to and apparently beyond 6 m. Release 11 was, however, an exceptional example. In other runs there was no apparent enrichment in CH_4 at 6 m. Nevertheless, it is evident that in these trials the gas cloud extended beyond a 1:10 height to fetch ratio and was closer to a ratio of 1:3.

3.7. Practical application

For the sake of practicality, it will be quite difficult to extend measurement heights beyond 10 m, which by our criterion would correspond to a maximum fetch of 30 m. This is an important finding for real on-farm applications of the MMD technique, where we expect that the CH_4 sources, be they animals, manure piles, lagoons or buildings, will usually extend more than 12 m upwind. Alternative approaches such as backward Lagrangian stochastic (bLS) models (e.g. the model proposed by Flesch et al., 1995; Crenna, 2004, personal communication) may be the solution to this problem. Theoretically, the use of such models permits emission rates to be calculated by making measurements of wind speed, and upwind and downwind concentrations at one height. This would eliminate the potential need for measurements to be made several metres above the ground, although further testing of the accuracy of bLS models is still required.

Another point to consider with regard to gas recovery is that area sources on the farm will occupy more space than the release grid used in these trials. Consequently, the path length will need to be longer. Given that the path length could be 200 m without loss in precision, and the minimum detectable concentration decreases as the path length increases, this may not be a problem. However, in many on-farm situations, it will usually be quite difficult to have a path length that long because of the need to have a clear "line of sight" for the laser and an unobstructed fetch for the wind profiles.

3.8. Performance in on-farm scenarios

Mature dairy cows produce about 0.38 kg $CH_4\,day^{-1}$. That rate corresponds to the production of 4.4 mg $CH_4\,s^{-1}$. The lowest release rate in these trials was 11.4 mg $CH_4\,s^{-1}$, equivalent to the production of two to three cows. The recovery from this trial was only 76%, but it is believed that the low value is a result of both a failure to establish accurate background concentrations during the release and from inadequate sensitivity in the laser system. The concentration at 4 m during the release was less than the estimated background, and the maximum enrichment in CH_4 (at 0.4 m) was only 7% greater than the background. Enrichment at 2 m was only 0.03 ppmv, which is just above the nominal sensitivity of the system of 0.02 ppmv. Fig. 8 is a plot of % recovery against class of release rate for a 10° exclusion angle. It indicates that the minimum sample size should be closer to ten animals (total release near 40 mg $CH_4\,s^{-1}$) rather than two or three. For release rates in excess of 40 mg $CH_4\,s^{-1}$, the mean recovery rate was 106% with a standard error of 4%. Allowing for the slight overestimation of recoveries discussed previously, the latter figure indicates that with sufficient replication

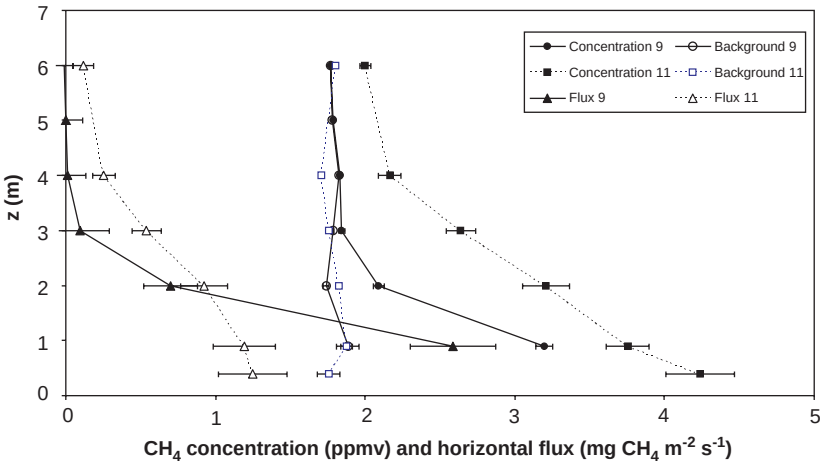

Fig. 7. Backgrounds, concentrations and horizontal fluxes with standard error bars during release 9 (near-neutral conditions; $L = -430$ m) and release 11 (highly unstable conditions; $L = -3.5$ m).

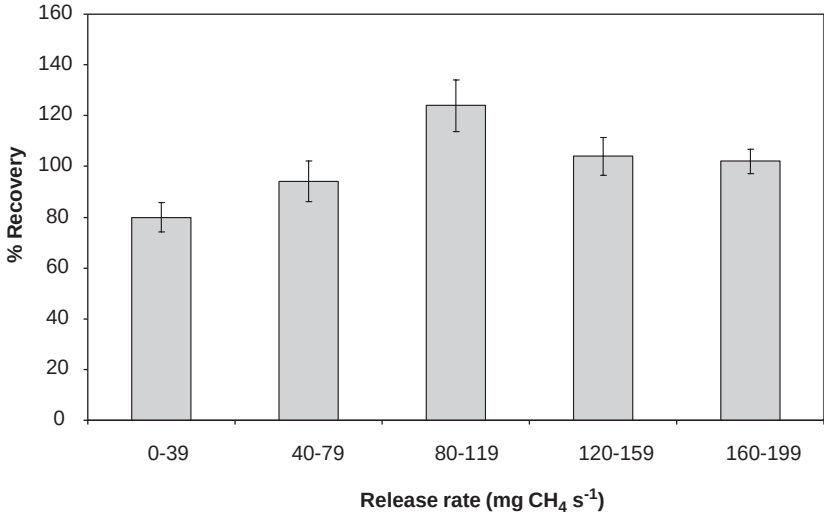

Fig. 8. Plot of % recovery against release rate by class with standard error bars based on a 10° exclusion angle.

(as in these trials), the system could detect a 9% change in production rate at the 5% probability level.

4. Conclusions

The paper reports the results of preliminary trials of a new technology for measuring CH_4 emissions. The technique involves the use of sonic anemometers and an open-path laser to measure the instantaneous rate at which CH_4 is transported by the wind away from the source. Trials of the method were conducted in a field within the Central Experiment Farm of AAFC in Ottawa, Canada in September 2002. Releases of CH_4 were made from cylinders via a mass flow controller to a ground-level grid, 3×3 m. Recoveries by the method were determined using a downwind laser path of 50.5 m with measurements of wind speed and CH_4 concentration at six heights up to 6 m. The nominal resolution of the laser system was 0.02 ppmv. Recoveries and various points of technique were explored in 23 releases. The main outcomes were:

- Recoveries calculated from instantaneous measurements of wind speed and concentration were 5% less than those calculated from the corresponding means over the same period. The latter overestimate the true emission rates.
- Recoveries sometimes exceeded 100%. This could indicate an error in the purity of CH_4 in the release cylinder, an error in the calibrations of the mass flow controller, errors in the calibration of the anemometers, errors in the calibration of the laser, or insufficient definition in the concentration and wind speed profiles.
- Because the increases in CH_4 concentration are small relative to the background, even when mimicking the production rate of 40 cows, it would be preferable to measure backgrounds simultaneously with the releases rather than in periods before and after release. This will be a necessary procedure in real animal trials.
- Changes in wind direction and lateral diffusion of the gas cloud between the release point and the laser path necessitate a criterion for excluding observations made when wind directions are outside certain preset limits. Excluding data when the wind trajectory was within 10° of the ends of the laser path, or outside them, was found to be a suitable criterion. It gave a mean recovery of 100% with a 5% confidence interval of 10% and excluded only 9% of the data.
- Practical difficulties in extending the trials to on-farm situations were seen to be the needs to have clear "lines of sight" for the laser, an unobstructed fetch for the wind profiles, and measurement heights higher than 6 m.
- Because of the difficulty in measuring small changes in concentration, it was concluded that the minimum sample size in animal trials would be ten dairy cows, producing about 40 mg $CH_4\,s^{-1}$.

The study has shown that the new technique can identify changes of 10% in CH_4 emission rates provided the rate is high enough and there is sufficient replication (as in this experiment). As discussed above, it has also identified a number of potential weaknesses in the present technique. Attention to these should improve precision and help in achieving the eventual aim of the work: to be able to measure changes in emission rates as small as 5%. In theory, the mass balance approach to

measuring fluxes is probably the best technique to apply where the field situation allows its use. It would be a preferred method because it is "model free" and has few assumptions. However, evaluation of the utility of an additional technique, the backward Lagrangian stochastic dispersion analysis method, may provide a simpler approach to apply in real animal trials and is seen as a potentially very useful exercise.

Acknowledgements

We wish to thank Louis-Olivier Savard and Jeff Scarbrough (USDA) for their assistance in field and Tom Flesch and Larry Mahrt for their assistance with the data analysis.

References

Bauer, J., 2004. Personal communication. Technical support specialist, Boreal Laser Inc, Spruce Grove, Alberta, Canada.

Blaxter, K.L., Clapperton, J.L., 1965. Prediction of the amount of methane produced by ruminants. British Journal of Nutrition 19, 511–522.

Crenna, B., 2004. Personal communication, Software developer, Thunder Beach Scientific, Halifax, Nova Scotia, Canada

Denmead, O.T., Harper, L.A., Freney, J.R., Griffith, D.W.T., Leuning, R., Sharpe, R.R., 1998. A mass balance method for non-intrusive measurements of surface-air trace gas exchange. Atmospheric Environment 32, 3679–3688.

Denmead, O.T., Leuning, R., Griffith, D.W.T., Jamie, I.M., Esler, M.B., Harper, L.A., Freney, J.R., 2000. Verifying inventory predictions of animal methane emissions with meteorological measurements. Boundary-Layer Meteorology 96, 187–209.

Desjardins, R.L., Allen JR., L.H., Lemon, E.R., 1978. Variations of carbon dioxide, air temperature, and horizontal wind within and above a maize crop. Boundary-Layer Meteorology 14, 369–380.

Flesch, T., Wlson, J.D., Yee, E., 1995. Backward time Lagrangian stochastic dispersion models, and their application to estimate gaseous emissions. Journal of Applied Meteorology 34, 1320–1332.

Harper, L.A., Denmead, O.T., Freney, J.R., Byers, F.M., 1999. Direct measurements of methane emissions from grazing and feedlot cattle. Journal of Animal Science 77, 1392–1401.

IPCC, 1996. In: Houghton, J.T., Meira Filho, L.G., Lim, B., Treanton, K., Mamaty, I., Bonduki, Y., Griggs, D.J., Callander, B.A. (Eds.), Intergovernmental Panel on Climate Change Greenhouse Gas Inventory Reference Manual, Revised IPCC Guidelines for National Greenhouse Gas Inventories, Vol. 3. OECD/ODCE, Paris.

IPCC, 2001. Climate Change 2001: The Scientific Basis. In: Houghton, J.T., Ding, Y., Griggs, D.J., Noguer, M., van der Linden, D.J., Dai, X., Maskell, K., Johnson, C.A. (Eds.), Contribution of Working Group I to the Third Assessment Report of the Intergovernmental Panel on Climate Change. Cambridge University Press, Cambridge, pp. 279–287.

Johnson, K.A., Huyler, H., Westberg, H., Lamb, B., Zimmerman, P., 1994. Measurement of methane emissions from ruminant livestock using a SF_6 tracer technique. Environmental Science and Technology 28, 359–362.

Judd, M.J., Kelliher, F.M., Ulyatt, M.J., Lassey, K.R., Tate, K.R., Shelton, I.D., Harvey, M.J., Walker, C.F., 1999. Net methane emissions from grazing sheep. Global Change Biology 5, 647–657.

Kaimal, J.C., Wyngaard, J.C., Izumi, Y., Cote, O.R., 1972. Spectral characteristics of surface layer turbulence. Quarterly Journal of the Royal Meteorological Society 98, 563–589.

Leuning, R., Freney, J.R., Denmead, O.T., Simpson, J.R., 1985. A sampler for measuring atmospheric ammonia flux. Atmospheric Environment 19, 1117–1124.

Leuning, R., Baker, S.K., Jamie, I.M., Hsu, C.H., Klein, L., Denmead, O.T., Griffith, D.W.T., 1999. Methane emission from free-ranging sheep: a comparison of two measurement methods. Atmospheric Environment 33, 1357–1365.

List, R.J., 1951. Smithsonian Meteorological Tables, 6th ed. Smithsonian Institution, Washington, DC.

Lockyer, D.R., Jarvis, S.C., 1995. The measurement of methane losses from grazing animals. Environmental Pollution 90, 383–390.

Miller, W.H., Koes, R.M., 1988. Construction and operation of an open-circuit indirect calorimetry system for small ruminants. Journal of Animal Science 66, 1042.

Paulson, C.A., 1970. The mathematical representation of wind speed and temperature profiles in the unstable atmospheric surface layer. Journal of Applied Meteorology 9, 857–861.

Thom, A.S., 1975. Momentum, mass and heat exchange of plant communities. In: Monteith, J.L. (Ed.), Vegetation and the Atmosphere, Vol. 1. Academic Press, London, pp. 57–109.

Wagner-Riddle, C., Park, K.-H., Thurtell, G.W., 2004. A micrometeorological mass balance approach for greenhouse gas flux measurements from stored animal manure. Agriculture and Forest Meteorology, in press.

Venkatram, A., 2004. On estimating emissions through horizontal fluxes. Atmospheric Environment 38, 1337–1344.